

**COMPOSITION, MICROPHYSICAL STATE, AND ENERGY BALANCE OF THE MARS SEASONAL POLAR CAPS FROM MGS.** G. B. Hansen, Hawaii Institute of Geophysics and Planetology, SOEST, University of Hawaii, 2525 Correa Road, Honolulu, HI 96822 ghansen@pgd.hawaii.edu.

**Introduction:** Continuing studies of the radiative properties of the seasonal polar caps of Mars will show how they impact the planetary energy balance and the seasonal cycle of CO<sub>2</sub>. These properties will be inferred by measurements from the Mars Global Surveyor (MGS), including primarily spectra and bolometric radiances from the thermal emission spectrometer (TES), but also reflectivity and cloud/surface detection from the Mars orbiter laser altimeter (MOLA) and images from the Mars orbiter camera (MOC). The shortwave measurements of the solar bolometer of TES and MOC images are available only for sunlit polar caps, while the 1- $\mu$ m MOLA observations are available for polar night as well, albeit only for a limited range of spacecraft altitudes and geometries. The TES spectra and thermal bolometer are usable over a wide range of altitudes and all lighting conditions. A study has already been completed using MOLA brightness data and TES spectra from two of the first 36 orbits to estimate the composition and grain size of both seasonal polar caps [1].

**Observation Details:** Observations are currently available from the “assessment subphase” (orbits 19–36, October 13 to November 7, 1997, seasonal dates  $L_S=197.4\text{--}213.6^\circ$ , available summer 1998), and part or all of the “science phasing” orbits, in two parts, SPO-1 and SPO-2, before and after solar conjunction (SPO-1, orbits 202–268, March 27 to April 28, 1998,  $L_S=299.7\text{--}318.9^\circ$ , and SPO-2, orbits 329–573, May 28 to September 23, 1998,  $L_S=335.1\text{--}33.4^\circ$ , both available in 1999). As of this writing, complete MOC images are available to orbit 50, complete TES data is available from orbits 19–36 and 214–268 (SPO-1) and complete MOLA data is available to the end of SPO-2.

**TES:** TES spectra are the primary tool for abundance, composition, and temperature determination. TES is composed of a Michelson interferometer measuring from 1650 to 200  $\text{cm}^{-1}$  ( $\sim 6\text{--}50\ \mu\text{m}$ ) with a finest spectral resolution of either 6 or 12  $\text{cm}^{-1}$ , and a two-channel bolometric radiometer measuring solar (0.3–2.7  $\mu\text{m}$ ) and thermal (5.5–100  $\mu\text{m}$ ) spectral regions [2]. It is equipped with a pointing mirror that was used in the large, elliptical early orbits to construct of spectral images (at low spatial resolution,  $\sim 130\ \text{km}$ ) of the disk of Mars. The finest spatial resolution of TES measurements is  $<3\ \text{km}$  [3]. Observations of the polar regions are useful only above 8–10  $\mu\text{m}$ .

**MOLA:** MOLA is used for surface reflectance and surface/cloud location determination. The primary pur-

pose of MOLA is to measure the planetary radius and topography using a pulsed laser system operating at a wavelength of 1.064  $\mu\text{m}$  [4]. Secondary products include the backscattered energy, and limited information on the width of the returned pulse, related to surface slope and roughness, and atmospheric scattering. For relative topography, the surface along-track resolution is  $\sim 300\ \text{m}$  and the vertical resolution is about 30 cm [5]. Optically thick clouds will generate a return near the cloud top, but the thin clouds typical of Mars will tend to scatter the pulse out of the forward direction, thus preventing a significant return.

**MOC:** MOC images will be used to determine the relative reflectance and distribution of seasonal deposits. Images in the mapping orbit have spatial resolutions of  $<2\ \text{m}$  for the narrow-angle camera and  $>200\ \text{m}$  for the wide-angle red and blue cameras [6]. The images in the elliptical orbits are of lower resolution, and are not typically concurrent with TES measurements [7].

**Previous Work:** The seasonal polar caps of Mars are composed primarily of solid CO<sub>2</sub>, and the optical properties of CO<sub>2</sub> ice require that pure snow with a sufficiently small particle size has a high visible/near-infrared albedo and a low infrared emissivity in parts of the thermal infrared, particularly in the region between 20 and 50  $\mu\text{m}$ . Dust mixed into or on top of the CO<sub>2</sub> ice will lower the visible albedo and bring the thermal infrared emissivity closer to 1. Water ice mixed with the CO<sub>2</sub> will have little effect in the visible and near-infrared to 1.4  $\mu\text{m}$  but can raise the 20–50  $\mu\text{m}$  emissivity if the particle size is  $>50\ \mu\text{m}$ . Observations of both seasonal polar caps during two of the assessment orbits of the Mars Global Surveyor spacecraft were used [1] to show that there is a strong correlation between visible brightness and low 20–50  $\mu\text{m}$  emissivity. TES spectra from regions with low 20–50  $\mu\text{m}$  brightness temperature are consistent with surface deposits of CO<sub>2</sub> with millimeter-sized grains and containing varying small amounts of dust, and they are not consistent with the expected signature of water ice or clouds. Large regions of low emissivity were seen in the spring south seasonal cap that had not been observed previously. They are correlated with visible bright regions (which are known to become brighter as the spring progresses) inferred from historical observations. In the north polar night, brightness is inferred from MOLA measurements. The model of seasonal CO<sub>2</sub> caps with bright, low-emissivity regions agrees

with previous visible observations of bright crater rims, streaks, and other bright areas within the polar caps, some of which may evolve into dark, high-emissivity sheet ice or may have evolved from dark, high-emissivity ice into brighter, fractured, fine-grained ice layers. It is also in agreement with models of the CO<sub>2</sub> cycle, which require average polar cap emissivities <0.9.

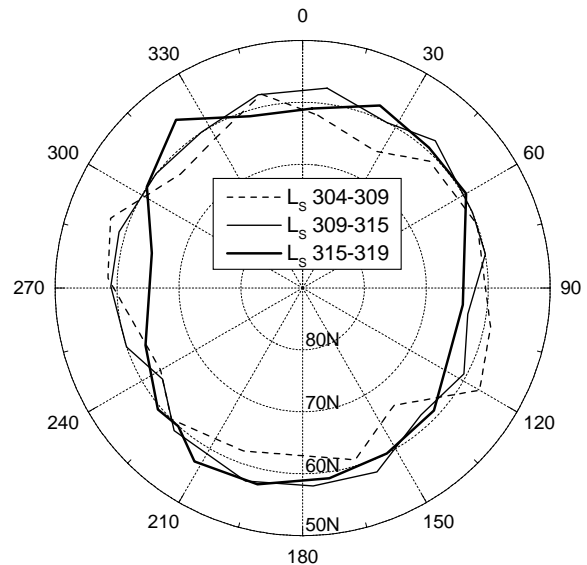
**New Work:** The goal of the new work is to expand on the previously analyzed data to include other orbits and other seasons, as available. For example, in SPO-1, TES observes the north polar seasonal cap at near its maximum size and the south polar cap near its minimum residual (CO<sub>2</sub>) size. The use of atmospheric models is necessary to separate the surface emission from that of the atmospheric gas and dust and to quantify the radiative contributions of the components to the whole.

**Surface models:** Simple radiative transfer codes are generally sufficient for modeling thermal emission. Optical constants for CO<sub>2</sub> ice and water ice are well enough known [1, and references therein], while those for dust can probably be improved from studies of dust in the atmosphere [8]. Intimate and spatial mixtures are easily modeled, while layered surface constructs require a more complex approach. The retrievable properties of the surface will include CO<sub>2</sub> grain size, amount of admixed dust or water ice, and surface temperature

**Atmospheric models:** A band model was developed for the earlier work [1] which is sufficient for modeling the 15- $\mu$ m CO<sub>2</sub> band in a clear atmosphere. The properties of dust and water ice aerosols can be readily modeled in the non-absorbing regions of the spectrum (given adequate optical constants for the dust [8]). The first approach for modeling the overlap region will be to include an infinitesimal aerosol layer at some level in an otherwise clear absorbing atmosphere. Ultimately, there will be a full correlated-k model [9] to handle absorbing and scattering aerosols in an absorbing atmosphere. The typical optical depths of atmospheric gas and aerosols will allow for the estimation of the surface radiance over a wide spectral range, even in the dusty southern spring conditions. Clouds of significant optical depth will be detectable by MOLA, which will aid in the TES interpretations.

**First results:** The SPO-1 TES spectra of the north polar seasonal cap show many very interesting features. The “surface temperature” quantity calculated by the TES team was compared to latitude and the lambert albedo from the visible bolometer for 51 passes over the north polar region. The temperature is based on the maximum brightness temperature over a restricted spectral range below 12.5 or between 20 and 33  $\mu$ m,

and can be strongly influenced by low emissivities from fine-grained CO<sub>2</sub> if temperatures from the longer wavelength region must be used. Hence, the value goes below 140 K in many places in the interior of the cap, even though surface temperatures probably are around 148 K. There is a clear correlation in most cases between bright spots in the sunlit margins of the cap and low “surface temperatures”, consistent with grain-size variations of the surface CO<sub>2</sub>. Much larger regions of cold temperatures in the cap interior will require comparison with MOLA data for interpretation. Observing the temperature near the margin for thermostatic behavior near 150 K allows for the mapping of the polar cap boundary [3, 10], which otherwise has not been estimated for seasons earlier than L<sub>S</sub>~330°. The continuous cap starts near 60°N throughout this interval (see Figure), with only small variations with season visible (agreeing with models [11]), and partial deposits extend to ~50°N.



#### References:

- [1] Hansen G. B. (1999) *JGR*, 104, (in press).
- [2] Christensen P. R. *et al.* (1992) *JGR*, 97, 7719–7734.
- [3] Christensen P. R. *et al.* (1998) *Science*, 279, 1692–1698.
- [4] Zuber M. T. *et al.* (1992) *JGR*, 97, 7781–7797.
- [5] Smith D. E. *et al.* (1998) *Science*, 279, 1686–1692.
- [6] Malin M. C. *et al.* (1992) *JGR*, 97, 7699–7718.
- [7] Malin M. C. *et al.* (1998) *Science*, 279, 1681–1685.
- [8] Snook K. J. *et al.* (1998) *BAAS*, 30, 1034.
- [9] Lacy A. A. and V. Oinas (1991) *JGR*, 96, 9027–9063.
- [10] Kieffer H. H. *et al.* (1998) *First Int. Conf. on Mars Polar Sci. and Explor.*, p. 23–24, LPI #953.
- [11] Wood S. E. and D. A. Paige (1992) *Icarus*, 99, 1–14.